Twisted Si=N Bonds: Matrix Isolation of Bridgehead Silanimines

Juliusz G. Radziszewski,[1a,b,*] Piotr Kaszynski,[1b] Dieter Littmann,[1b] V. Balaji,[1b,c] B. A. Hess, Jr.,[1d] and Josef Michl[1b,c,*]

Contribution from the Department of Chemistry and Biochemistry, University of Colorado at Boulder, Boulder, Colorado 80309-0215, Laser Spectroscopy Facility, Department of Chemistry, University of California, Irvine, California 92717, and Department of Chemistry, Vanderbilt University, Nashville, Tennessee 37235

Received March 18, 1993

Abstract: We report the IR and UV–vis spectra of three bridgehead silanimines, 1-sila-2-azabicyclo[3.2.2]non-1(2)-ene, 1-sila-2-azabicyclo[3.2.1]oct-1(2)-ene, and 1-sila-2-azabicyclo[2.2.2]oct-1(2)-ene, prepared in matrix isolation by UV irradiation of bridgehead silyl azide precursors and characterized by chemical trapping with trimethoxymethylsilane with and without prior selective photodestruction with light of suitable wavelengths. The IR spectra of the ^{14}N and ^{15}N species and the n → π* transition in their UV–vis spectra are in good agreement with *ab initio* computations. It is concluded that π bonding plays a crucial role in determining the properties of silanimines.

Introduction

The nature of multiple bonds to silicon has been of considerable interest in recent years,[2,3] and the Si=N double bond has been no exception. This is clearly a very polar bond and has been at times written in the zwitterionic silicenium ylid form, $Si^+–N^-$.[4] Indeed, the silicon atom acts as if it were coordinatively unsaturated, and stable adducts of silanimines carrying bulky protecting groups with Lewis bases have been isolated.[5] However, the Si=N bond length in a free silanimine stabilized by bulky substituents is fully 0.1 Å shorter than a Si–N single bond length[6] and corresponds to expectations for a true double bond. The presence of π bonding and high bond polarity are also shown by results of quantum chemical computations.[7]

A direct way to probe the effects of π bonding on the properties of the Si=N bond would be to examine molecules with twisted Si=N bonds. In these, π bonding would be significantly weakened. An obvious choice is small-ring bridgehead silanimines, and we have selected **1**, **2**, and **3** as suitable targets.

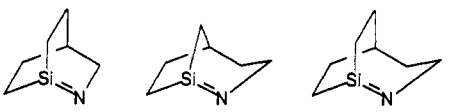

1 **2** **3**

Ours is not the first study of these bridgehead silanimines. In 1981, Elseikh and Sommer reported an investigation of the photochemical decomposition of 1-azido-1-silabicyclo-[2.2.1]heptane (**4**) and 1-azido-1-silabicyclo[2.2.2]octane (**5**) in room-temperature cyclohexane solution in the presence of a trapping agent, trimethoxymethylsilane.[8] The trapping products **6** and **7**, respectively, were isolated, and transient formation of the bridgehead silanimines **1** and **3** was postulated. Surprisingly, the adduct **8** was not detected in the reaction of **4**, and it thus appeared that the irradiation of **4** yielded only **1** to the exclusion of **2**.

We have now repeated the work of Elseikh and Sommer[8] and found that **8** is formed, after all. Subsequently, we have investigated the photochemistry of **4** and **5** under conditions of argon matrix isolation and observed the formation of **1**, **2**, and **3** (Schemes I and II), and in the following, we describe their spectral characteristics. They provide a very eloquent testimony to the importance of the π component in the Si=N bond.

Results

Synthesis of Precursors. The azides **4** and **5** were prepared according to the literature procedures[8] from the corresponding silyl chlorides **9**[9] and **10**.[10] The chlorides **9** and **10** were synthesized starting from tetrahydropyran-4-carboxylic acid[11] (**11**) obtained from diethyl malonate[11–14] (Scheme III). The acid was converted to 4-(bromomethyl)tetrahydropyran[15] (**12**), which in turn served as a precursor to 4-(2-bromoethyl)tetrahydropyran[16,17] (**13**). The bromide **13** was substituted for the analogous chloride used in the original synthesis[10] of the silyl chloride **10**. The chlorides **9** and **10** were obtained from the bromides **12** and **13** via the trichlorides **14** and **15** and the pentachlorides **16** and **17** in a procedure analogous to that described[18] in detail for the preparation of 1-chloro-1-silabicyclo[2.2.2]octane (**10**). The overall transformations are shown in Scheme III.

Room-Temperature Irradiation and Trapping Experiments. The reported[8] room-temperature irradiation of the azides **4** and **5** and

(1) (a) University of California. (b) Large parts of this project were completed while the authors were at the University of Utah and The University of Texas at Austin. (c) University of Colorado. (d) Vanderbilt University.
(2) Raabe, G.; Michl, J. *Chem. Rev.* **1985**, *85*, 419.
(3) Raabe, G.; Michl, J. In *The Chemistry of Organic Silicon Compounds*; Patai, S., Rappoport, Z., Eds.; John Wiley & Sons Ltd.: Chichester, U.K., 1989; Chapter 17, p 1015.
(4) E.g.: Klingebiel, Y.; Meller, A. *Z. Naturforsch.* **1977**, *32B*, 537.
(5) Wiberg, N.; Schurz, K. *J. Organomet. Chem.* **1988**, *341*, 145. Wiberg, N.; Schurz, K. *Chem. Ber.* **1988**, *121*, 581. Boese, R.; Klingebiel, U. *J. Organomet. Chem.* **1986**, *315*, C17.
(6) Wiberg, N.; Schurz, K.; Reber, G.; Müller, G. *J. Chem. Soc., Chem. Commun.* **1986**, 591.
(7) (a) Truong, T. N.; Gordon, M. S. *J. Am. Chem. Soc.* **1986**, *108*, 1775. (b) Schleyer, P. v. R.; Stout, P. D. *J. Chem. Soc., Chem. Commun.* **1986**, 1373.
(8) Elseikh, M.; Sommer, L. H. *J. Organomet. Chem.* **1980**, *186*, 301.
(9) Sommer, L. H.; Bennett, O. F. *J. Am. Chem. Soc.* **1957**, *79*, 1008.
(10) Sommer, L. H.; Bennett, O. F. *J. Am. Chem. Soc.* **1959**, *81*, 251.
(11) Hanousek, V.; Prelog, V. *Collect. Czech. Chem. Commun.* **1932**, *4*, 259.
(12) Burger, A. *Chem. Abstr.* **1946**, *40*, 5455.[8]
(13) Stanfield, J. A.; Daugherty, P. M. *J. Am. Chem. Soc.* **1959**, *81*, 5167.
(14) Tamura, F.; Uehara, K.; Ito, Y.; Murata, N. *Chem. Abstr.* **1965**, *63*, 16479c.
(15) Burger, A.; Turnbull, L. B.; Dinwiddie, J. G., Jr. *J. Am. Chem. Soc.* **1950**, *72*, 5512.
(16) Kolbach, D.; Rill, M.; Cerkovnikov, E. *Acta Pharm. Jugosl.* **1956**, *6*, 65; *Chem. Abstr.* **1957**, *51*, 8082g.
(17) Prelog, V.; Kohlbach, D.; Cerkovnikov, E.; Rezek, A.; Piantanida, M. *Liebigs Ann. Chem.* **1937**, *532*, 69.
(18) Cunico, R. F.; Drone, F. *J. Organomet. Chem.* **1978**, *150*, 179.

0002-7863/93/1515-8401$04.00/0

Scheme I

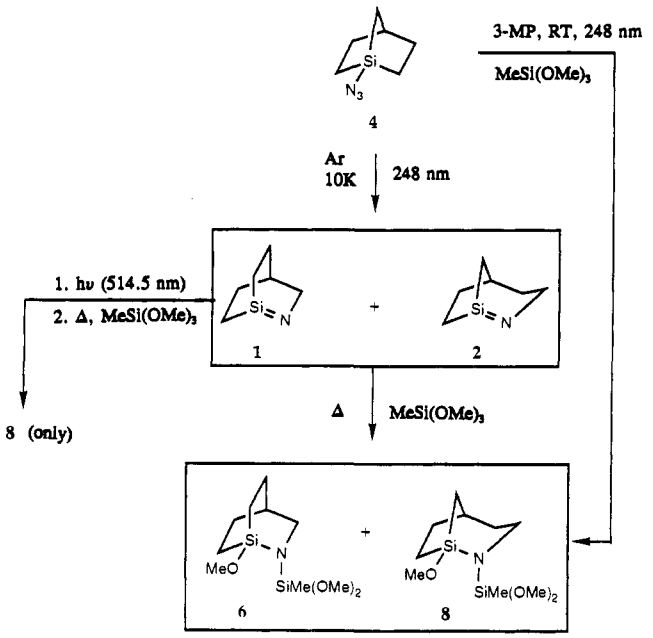

Scheme II

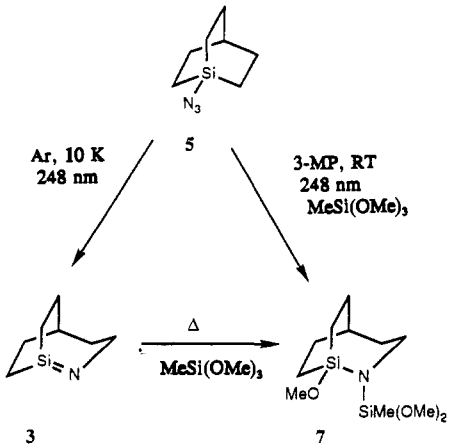

Scheme III

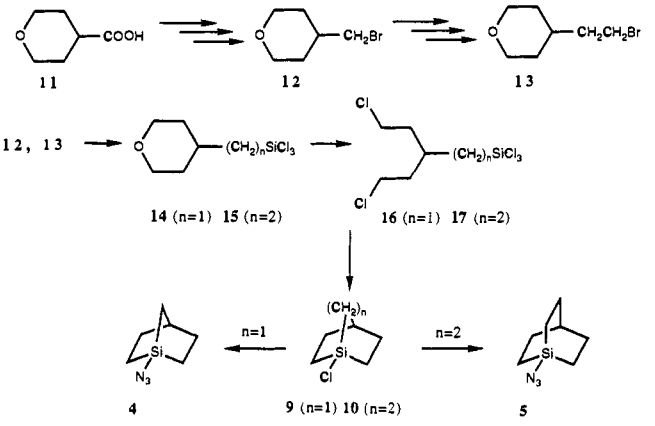

trapping of the imines **1** and **2** as adducts **6** and **7** have been repeated. However, we have now also detected the adduct **8**, implicating the intermediate imine **2**.

A solution of the azide **4** in cyclohexane containing trimethoxymethylsilane was irradiated with 248-nm KrF excimer laser light for several hours. The major component of the resulting reaction mixture was separated by preparative GC and analyzed by NMR spectroscopy and capillary column GC. Contrary to the

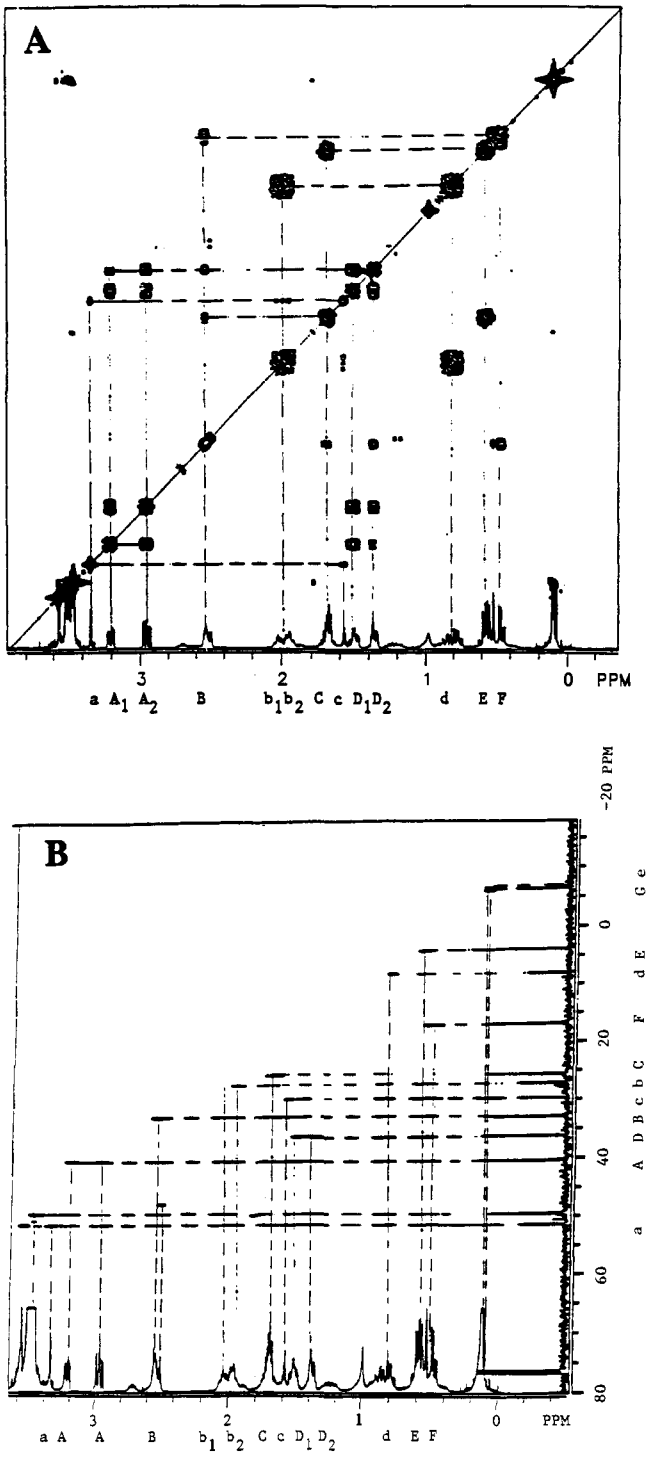

Figure 1. Spectra of the isolated mixture of **6** (lower case letters) and **8** (upper case letters). A: 2D ^1H–^1H NMR. B: 2D ^1H–^{13}C NMR.

previous report,[8] the isolated product was found to be a mixture of the two isomers **6** and **8** in a ratio of about 1:3 (Scheme I). The components of this oily moisture-sensitive mixture have very close GC retention times even on capillary columns, making the failure of the earlier authors to detect them separately understandable, and making a preparative separation extremely difficult. Fortunately, the separation was not needed for our purposes.

The proton and carbon chemical shifts of the individual isomers in the mixture have been unambiguously assigned on the basis of 2D ^1H–^1H and 2D ^{13}C–^1H spectra (Figure 1). The key point of the analysis was the recognition of three sets of multiplets (δ 2.95, 3.20, and 3.35) characteristic for hydrogens of the CH_2–N

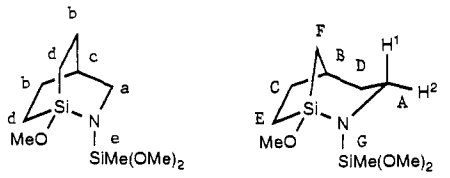

6 8

Figure 2. Assignment of chemical shifts to skeletal hydrogens and carbons in **6** and **8**.

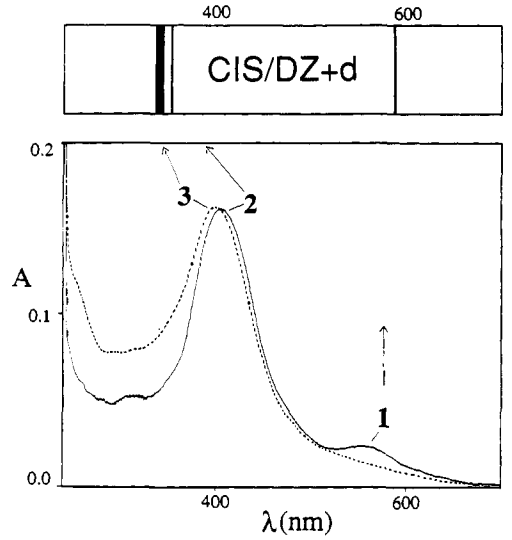

Figure 3. UV–vis absorption spectra of argon matrix isolated **3** (dashed line) and mixture of **1** and **2** (solid line). Intensities in both curves are arbitrarily scaled. On top are spectra calculated at the CIS/DZ+d level for Me_2Si=NMe distorted to the geometries of **1**, **2**, and **3**. (The oscillator strength for the thin lines is 0.01, and for the thick line, 0.07.)

group. The first two multiplets (A_1 and A_2, δ 3.20 and 2.95, respectively) are coupled with each other and are also related to six other multiplets (B–F) assigned to the skeletal hydrogens. This brings the total number of distinct hydrogens up to eight. The third multiplet (a) at 3.35 ppm is related to only four other multiplets (b–d) in the region of the skeletal hydrogens, and thus the total number of the distinct hydrogens in this set is five. On the basis of the symmetry of the expected products, the first set of the multiplets (A–F) can be assigned to the less symmetrical compound **8**, and the second set (a–d), to the more symmetrical product **6**. The chemical shifts of the skeletal hydrogens in **6** and **8** are assigned on the basis of the δ values and the separations between the groups of hydrogens. The ^{13}C NMR shifts of the skeletal carbons were easily assigned on the basis of a 2D ^1H–^{13}C NMR correlation (Figure 1B). The signals of methyl and methoxy hydrogens and methoxy carbons in **6** and **8** are not well resolved. The NMR assignments are summarized in Figure 2. Integration of distinct multiplets (e.g., $-CH_2N-$ and the bridgehead CH) in the proton NMR spectrum of the mixture of **6** and **8** has shown that the latter is the major isomer.

The azide **5** was photodecomposed similarly in the presence of trimethoxymethylsilane and cleanly produced the adduct **7** (Scheme II). The compound was isolated by preparative GC and characterized by high-field ^1H and ^{13}C NMR spectroscopy, confirming the previous results.[8]

Matrix-Isolation Photochemistry and Spectroscopy. 1-Azido-1-silabicyclo[2.2.2]octane (5). Irradiation of **5** isolated in an Ar matrix at 10 K with 248-nm light gradually destroyed its electronic absorption band (λ_{max} = 270 nm). At the same time, a new absorption band at 397 nm grew in (Figure 3). Concurrently, the IR spectrum of the azide was replaced by a new set of peaks. Light of wavelengths longer than 350 nm converted this initial photoproduct to a secondary photoproduct, as evidenced by the

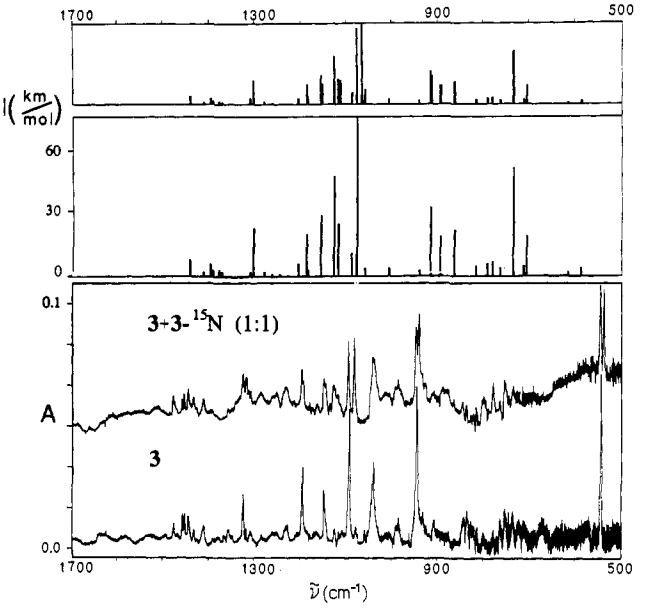

Figure 4. Infrared absorption spectrum of **3** (bottom) and of a 1:1 mixture of **3** and **3**-^{15}N (above) in the Ar matrix (12 K). The top two graphs represent spectra calculated for **3** and **3** + **3**-^{15}N (1:1) at the RHF/6-31G* level. The computed frequencies were scaled by a factor of 0.86.

replacement of its peaks in the IR spectrum by another set of peaks.[19] Such experiments, combined with computer subtraction of spectra, yielded the IR spectra of the unlabeled and the partially ^{15}N-labeled primary photoproduct (Figure 4), to which we assign the expected structure **3** on the basis of a chemical trapping experiment in an argon matrix coated with $MeSi(OMe)_3$.

When such a matrix was warmed to room temperature after the primary photoproduct had been generated, GC–MS analysis revealed the presence of the expected trapping product **7**, confirmed by comparison with an authentic sample obtained in the room-temperature experiment described above. However, when in a separate experiment the matrix was warmed only after the 397-nm band of the primary photoproduct had been bleached completely with longer wavelength light (>350 nm), **7** was not detectable.

The position of the UV absorption peak at 397 nm is compatible with the vertical excitation energy obtained by *ab initio* calculations for a suitably distorted model molecule, Me_2Si=NMe, at the level of CI (singles) with a DZ+d basis set (Figure 3). The geometry of the model chromophore was chosen so as to mimic the geometry of **3** optimized at the RHF/6-31G* level: the C, Si, and N atoms were held fixed at the locations optimized for **3**, while the positions of the nine hydrogen atoms of the methyl groups in Me_2Si=NMe were optimized.

A comparison of the IR spectrum of the primary photoproduct, including the isotopic shifts, with the spectral frequencies and shifts calculated for **3** at the *ab initio* RHF/6-31G* level and scaled by a uniform factor of 0.86 supports the structural assignment (at this level of approximation, the calculated intensities are not considered reliable). The comparison (Figure 4) identifies the Si=N stretching vibration with an IR peak at 1088 cm^{-1} (calculated, 1076 cm^{-1}), which exhibits a ^{15}N shift of

(19) (a) The peaks of the secondary photoproduct from **5** are located at 1668 (1648), 1488 (1479), 1369, 1152, 966 (960), 915, 855, 828, 809, and 766 cm^{-1} for the ^{14}N- (^{15}N-) containing sample. This secondary photoproduct was not investigated further. Its IR spectrum suggests that it may be the imine expected from a 1,3 sigmatropic shift in **3**, *N*-(1-silabicyclo[2.1.1]hex-1-yl)formaldimine. (b) The observed peaks of the two secondary photoproducts from **4** were weaker, and we are less sure of their location. Irradiation of the 557-nm primary product appears to yield the strongest peaks at 1666 (^{14}N) and 1648 (^{15}N) cm^{-1}; irradiation of the 406-nm primary product appears to yield the strongest peaks at 1668 (^{14}N) and 1649 (^{15}N) cm^{-1}. These values suggest that the photochemical destruction of these silanimines also involves 1,3 shifts to substituted formaldimines.

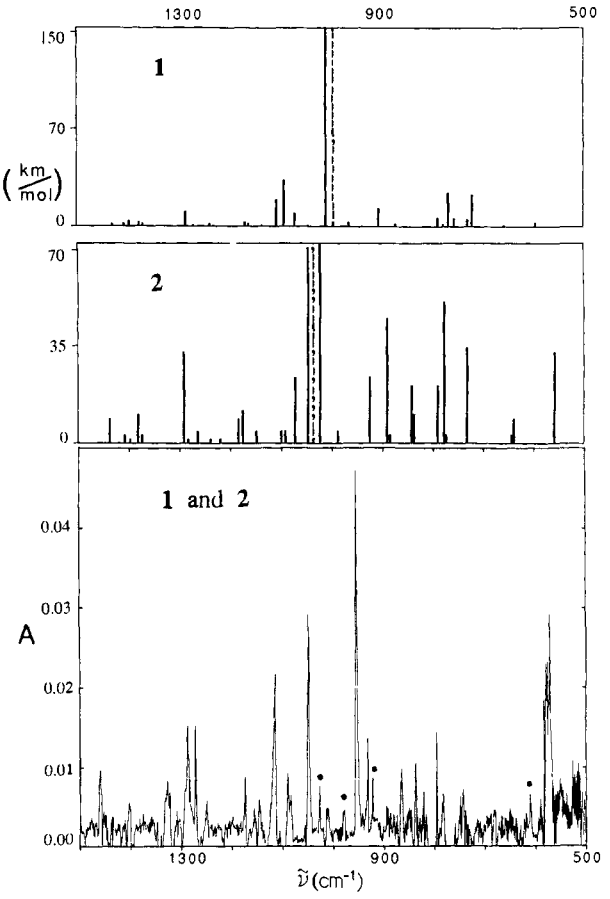

Figure 5. Infrared absorption spectrum of the mixture of **1** and **2** isolated in the Ar matrix (12 K). The bands due to **1** are marked with dots. Above are the calculated spectra for **1** and **2** (RHF/6–31G*); frequencies were scaled by 0.86. The dashed lines indicate the Si=N stretching vibrations computed for ^{15}N-labeled molecules.

11 cm^{-1} (calculated, 11 cm^{-1}). Only one other intense IR band showed a significant nitrogen isotopic shift. This was a peak at 943 cm^{-1}, shifted to 936 cm^{-1} in the ^{15}N compound. It probably has significant C–N stretching character.

1-Azido-1-silabicyclo[2.2.1]heptane (4). In this instance, lower molecular symmetry suggests that two isomeric bridgehead silanimines could form in an approximately statistical ratio in the matrix as they did in the room-temperature solution trapping experiment. Indeed, this is the result observed. The separate structure proofs and spectroscopic characterization of the two isomeric primary photoproducts were greatly facilitated by the use of monochromatic laser light to perform selective photochemical transformations on the two isomers, whose UV–vis absorption spectra differ greatly.

Irradiation of **4** isolated in an Ar matrix with KrF excimer laser light at 248 nm rapidly decomposed it. Azide absorption (λ_{max} = 270 nm) was replaced by two new peaks in the visible region, a stronger one with a maximum at 406 nm and a much weaker one peaking at 557 nm (Figure 3). Concurrently, new absorptions appeared in the IR spectrum (Figure 5). When the matrix was coated with $MeSi(OMe)_3$, warm-up at this point produced the two adducts **6** and **8**, identified by capillary GC and 2D NMR as described above.

When a matrix containing the primary photochemical products was exposed for a short time to 514.5-nm light (Ar ion laser) in a separate experiment, the longer wavelength absorption band at 557 nm disappeared rapidly.[19] When this experiment was performed on a matrix coated with $MeSi(OMe)_3$, analysis of the trapping mixture after subsequent warm-up revealed only the adduct **8**. Longer broad-band visible irradiation destroyed also the other visible absorption band at 406 nm.[19] In such a case, subsequent warm-up of a matrix coated with the trapping agent did not yield either adduct in detectable amounts. On the basis of this evidence, we attribute the 557-nm peak to **1** and the 406-nm peak to **2**. This is also compatible with the results of our *ab initio* calculations for a suitably distorted model chromophore, $Me_2Si{=}NMe$, performed similarly as for **3** (Figure 3).

IR spectra of both species, unlabeled and partially ^{15}N-labeled, were obtained by computer subtraction of spectra recorded before and after the irradiation of the primary photoproduct mixture by 514.5-nm and broad-band visible light for **1** alone and **1** together with **2**, respectively. The spectra and the isotopic shifts agree well with the results of RHF/6–31G* calculations of vibrational frequencies and isotopic shifts (Figure 5). The results permit us to identify the frequencies of Si=N vibrations in both **1** and **2**. They are at 1014 cm^{-1} (**1**) and 1050 cm^{-1}(**2**) and are shifted to lower values by 16 and 8 cm^{-1}, respectively, in the ^{15}N-labeled compounds. The scaled calculated values are 1007, 1044, 15, and 9 cm^{-1}, respectively. Only one other intense IR peak in each compound showed a significant nitrogen isotopic shift. In **1**, it was located at 932 cm^{-1} (927 cm^{-1} with ^{15}N), and in **2**, at 955 cm^{-1} (948 cm^{-1} with ^{15}N). It probably belongs to a vibration with considerable C–N stretch character.

We were never able to accumulate large concentrations of **1** and **2** in the matrix, since both compounds are destroyed by the 248-nm light used for the irradiation of the azide precursor (**4**). The azide **4** seems to be inert to longer wavelength radiation (i.e., 308 nm).

Discussion

Photochemistry of Bridgehead Silyl Azides. The photochemical loss of N_2 from silyl azides, accompanied by a rearrangement to silanimines, is a general process that was established a long time ago[2,3] and requires little comment. Our results have solved the vexing puzzle[8] as to why the more stable isomer **2** is not formed upon irradiation of **4**. The answer is that **1** and **2** are both formed, and the reason why only the adduct **6** but not **8** was observed by the earlier workers is that they are nearly inseparable by GC. Their present separate identification illustrates the power of modern 2D NMR spectroscopy.

Our results support the standard belief[20] that the loss of N_2 is concerted with the rearrangement and that a singlet nitrene does not appear as a distinct intermediate. In the reaction of **4**, the less strained [3.2.1] bicyclic product **2** enjoys a statistical advantage by a factor of 2. Moreover, it is significantly more stable than the [2.2.2] bicyclic product **1**. In the RHF/6-31G* approximation, without correction for zero-point energies, the difference is 13 kcal/mol. It is hard to see how a thermally equilibrated singlet nitrene intermediate could fail to rearrange predominantly to **2** as opposed to **1**. Yet, assuming equal trapping efficiencies, **2** is formed in only about a 3-fold excess.

The regiochemistry of the rearrangement is most likely dictated by the conformation of the azide. With backside displacement, a minor deviation from a purely statistical distribution among the three staggered conformations in favor of the two in which one one-carbon bridge and one two-carbon bridge represent the flanking groups, which appears entirely reasonable, would then readily account for the approximate 1:3 product ratio. A similar situation was encountered earlier with analogous bridgehead azides derived from hydrocarbons.[21,22]

Bridgehead Silanimines 1–3. Geometry and Bonding. The chemical trapping experiments combined with selective photodestruction of a component in a mixture leave no doubt as to which UV–vis and IR spectra are to be attributed to which

(20) Nguyen, M. T.; Faul, M.; Fitzpatrick, N. J. *J. Chem. Soc., Perkin Trans. 2*, **1987**, 1289.
(21) Radziszewski, J. G.; Downing, J. W.; Wentrup, C.; Kaszynski, P.; Jawdosiuk, M.; Kovacic, P.; Michl, J. *J. Am. Chem. Soc.* **1984**, *106*, 7996.
(22) Radziszewski, J. G.; Downing, J. W.; Wentrup, C.; Kaszynski, P.; Jawdosiuk, M.; Kovacic, P.; Michl, J. *J. Am. Chem. Soc.* **1985**, *107*, 2799.

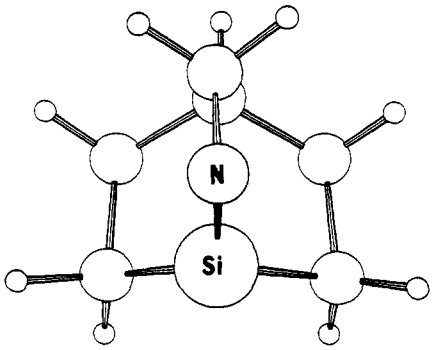

Figure 6. Calculated equilibrium geometry of **1** (RHF/6-31G*).

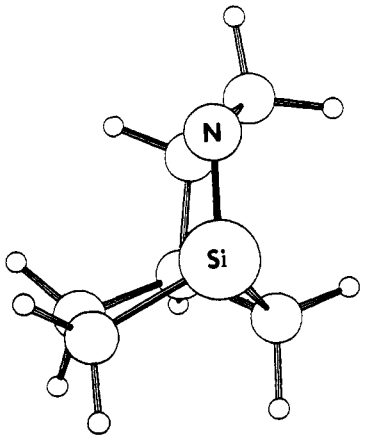

Figure 7. Calculated equilibrium geometry of **2** (RHF/6-31G*).

chemical structure. The agreement between the observed and the calculated IR and UV–vis spectra serves as an additional structural confirmation.

Of the two possible geometrical isomers of **2**, only one has been observed, and we presume that this is the more stable *Z* form shown in the formula. In the case of the carbon analogue, both the *Z* and the *E* forms were spectroscopically observable.[22] The latter was extremely photolabile and never accumulated in the matrix to an extent higher than about 5% of the *Z* form. It is quite possible that the *E* form of the silamine **2** was formed to a small degree in the present set of experiments as well but remained unobserved.

The geometrical structures of the silanimines are not known. In view of the good performance of the RHF/6-31G* calculations for the IR frequencies and isotopic shifts, it appears reasonable to assume that the calculated structures are nearly correct. They are shown in Figures 6–8.

The calculated lengths are longer by about 0.05 Å for the bridgehead Si=N bond lengths relative to the planar Me_2Si=NMe model (Table I), suggesting that the double bond is weakened by twisting. The 1.55-Å value in the planar model can be compared with the X-ray value of 1.568 Å determined[6] for the nearest known analogue, *t*-Bu_2Si=NSi-*t*-Bu_3. Unfortunately, a direct comparison is not reliable, since in the latter compound the valence angle at the nitrogen is nearly 180°, making its lone pair perfectly available for donation to the antibonding orbitals on the singly bonded silicon. Such linearization is known[7b] to shorten the Si=N distance, while silylation on the nitrogen extends it.

The three angles that are most important for the description of the deformation of the Si=N bond induced by the bicyclic skeleton are the Si pyramidalization angle ω, the nitrogen valence angle SiNC, and the twist angle θ (Table I). Large deviations of ω and θ from zero correspond to a weakened π component of the double bond. The calculated Si pyramidalization angles are rather small in **1** and **3** and significantly larger in **2**, presumably

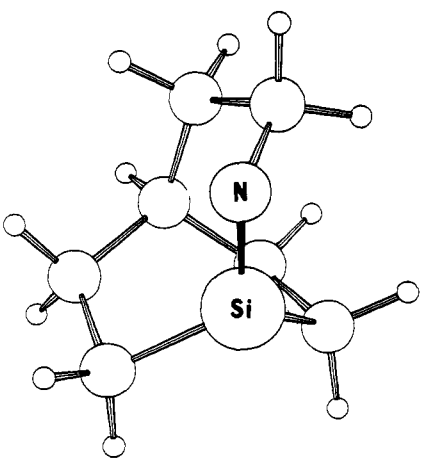

Figure 8. Calculated equilibrium geometry of **3** (RHF/6-31G*).

Table I. Geometries and Si=N Stretching Vibrations of Silanimines **1–3**

compound	$R_{Si=N}$[a] (Å)	θ[b] (deg)	ω[c] (deg)	SiNC[d] (deg)	$\tilde{\nu}_{Si=^{14}N}$[e] (cm^{-1})	$\tilde{\nu}_{Si=^{15}N}$[f] (cm^{-1})	$\Delta\tilde{\nu}$[g] (cm^{-1})
1 calcd[h]	1.596	82.0	13.8	98.9	1007	992	15
exptl					1014	998	16
2 calcd[h]	1.600	35.5	18.5	108.4	1044	1035	9
exptl					1050	1042	8
3 calcd[h]	1.592	47.3	13.7	110.6	1076	1065	11
exptl					1088	1077	11
Me_2Si=NMe[i] calcd[h]	1.551	0.0	0.0	150.4	1355	1326	29

[a] The Si=N bond length. [b] The twist angle at the Si=N bond, as defined by the dihedral angle between the axes of the Si and N orbitals participating in the π bond (on Si, this axis makes equal angles with the three bridgehead bonds, and on N, this axis is perpendicular to the SiNC plane). [c] The pyramidalization angle on Si, given by the amount by which the angle between the axis of the π-bonding Si orbital and any one of the three bridgehead bonds exceeds 90°. [d] The valence angle on N. [e] The Si=N stretching frequency in the ^{14}N molecule. [f] The Si=N stretching frequency in the ^{15}N molecule. [g] The ^{15}N isotopic shift. [h] The harmonic frequency computed at the RHF/6-31G* level and scaled by a factor of 0.86. [i] Computed results for Me_2Si=NMe are included for comparison.

weakening the π bond in the latter more than in the former two. The SiNC valence angles are all much smaller than in the unstrained Me_2Si=NMe. They are comparable in **2** and **3** and significantly smaller in **1**. The strong bending at the nitrogen atom does not affect the π bond directly but reduces the overall SiN bonding strength by inhibiting the donation of the N lone pair into the antibonding orbitals on the Si atom. However, the degree to which π bonding in the Si=N (or C=N) bond of an imine is reduced by twisting is a sensitive function of the valence angle on N. Clearly, for N valence angles close to 180°, there is hardly any reduction in π overlap and π bonding upon twisting at all, even at orthogonality (θ = 90°). As discussed for the C=N bond in some detail elsewhere,[23–25] even at the more usual N valence angles close to 120°, appropriate for nearly sp^2 hybridization, twisting to orthogonality does not break all π bonding but merely reduces it. The fully twisted (θ = 90°) C=N bond is analogous to a C=C bond strongly pyramidalized on one end, not to a C=C bond twisted to orthogonality. This is obvious once it is realized that a θ = 90° twist of a C=N (or Si=N) bond merely interchanges the role of the two valence orbitals used by the nitrogen atoms. In the ground state, a 2p orbital is used for π bonding and an sp^2 hybrid to hold a lone pair when θ = 0°, and the reverse is true when θ = 90°. Since a 90° twist does not remove the π component of an Si=N (or C=N) double bond,

(23) Michl, J.; Radziszewski, J. G.; Downing, J. W.; Kopecký, J.; Kaszynski, P.; Miller, R. D. *Pure Appl. Chem.* **1987**, *59*, 1613.
(24) Bonačić-Koutecký, V.; Michl, J. *Theor. Chim. Acta* **1985**, *68*, 45.
(25) Radziszewski, J. G.; Downing, J. W.; Jawdosiuk, M.; Kovacic, P.; Michl, J. *J. Am. Chem. Soc.* **1985**, *107*, 594.

the strength of this component cannot be estimated by computing the energy needed for such a twist, as is occasionally assumed in the literature,[7a] and other procedures[7b] are preferable. Thus, the value of 38 kcal/mol derived[7a] from the twisting energy, computed with MCSCF/6-31G* followed by second-order CI, represents a lower limit for the Si=N π bond strength in H_2Si=NH, and the value of 45 kcal/mol derived[7b] from isodesmic processes at the MP4/6-31G*+ZPE level is more meaningful.

Since, in the bridgehead silanimines **1–3**, the valence angle SiNC is forced to be relatively small by the bicyclic structure, the weakening of the π bond strength by twisting must be significant. The calculated twist angles θ are quite large and increase distinctly in the order Me_2Si=NMe, **2**, **3**, **1**. This is not the order in which ring size decreases regularly, and may appear counterintuitive. Molecular models suggest that the distortions in **2** and **3** should be comparable and do not provide a clue as to why the *trans*-1-azacycloheptene ring should have a less twisted double bond when bridged with a methylene group, as in **2**, than when bridged with an ethylene group, as in **3**. We note, however, that the order is the same as calculated earlier by the MNDO method for the analogous series of bridgehead imines with twisted C=N bonds (69°, 39°, and 48° for the analogues of **1**, **2**, and **3**, respectively).[23]

Since the calculated twist angle θ increases as one proceeds from **2** to **3** and further to **1**, while the pyramidalization angle ω increases in the order $\mathbf{1} \cong \mathbf{3} < \mathbf{2}$, it is not easy to make qualitative predictions of the SiN bond strength. This is exemplified by the computed Si=N bond lengths, which are nearly the same in all three bridgehead silanimines. Because of the huge twist angle in **1**, one could expect this silamine to have the lowest Si=N bond stretching frequency and the lowest n $\rightarrow \pi^*$ transition energy, but it is not very clear what to expect on qualitative grounds for a comparison of **2** and **3** from their computed structures alone.

Vibrational Spectra. Although the frequencies assigned to bond stretching vibrations reflect not only the bond stretching force constants but also the degree of coupling of the stretching motion with the remainder of the molecule, they are commonly used as a rough measure of bond strength. The large drop in the Si=N stretching frequency in **1–3** relative to MeSi=NMe (Table I) can be understood in this way and attributed to the much smaller SiNC valence angle as discussed above. The approximate nature of this measure of Si=N bond strength in the silanimines **1–3** is emphasized by the huge variation in the magnitude of the ^{15}N isotopic shift in Table I, which reflects the degree of coupling of the Si=N stretching motion with motions in the rest of the molecule. Viewed in this light, and recalling the opposite trends in θ and ω, it is not surprising that the Si=N bond stretching frequencies observed and computed in the series **1–3** do not follow the calculated twist angle θ in a simple way. Still, **1** appears to be in a class apart, and there is little doubt that the reduction of the π component of the bonding by the very large twisting weakens the Si=N bond in this molecule noticeably. Once again, the higher observed and computed Si=N frequency in **3** relative to **2** is analogous to the higher observed and computed C=N frequency in their carbon analogues (1480, 1586, and 1597 cm^{-1} observed for the analogues of **1**, **2**, and **3**, respectively).[23]

Electronic Spectra. The huge change in the lowest singlet excitation energy in the series **1–3** (Figure 3, Table II) alone leaves no doubt that twisting has a profound effect on the electronic structure of the Si=N chromophore. However, hardly any difference is observed or calculated between the n $\rightarrow \pi^*$ transitions in **2** and **3**, and the opposed effects of the differences in ω and θ apparently largely cancel. Again, **1** is in a class by itself.

As discussed for the analogous twisted C=N chromophore in detail elsewhere,[23-25] the twisted Si=N chromophore is isoelectronic with an allyl anion twisted about its C—C bonds to various degrees. Two of its three principal orbitals are doubly occupied in the ground state, one is empty. According to a detailed MRD-CI study of H_2Si=NH,[26] the orbital ordering is n, π, and π^* in the order of increasing energy at the planar equilibrium geometry, with the n and π orbitals close in energy. This corresponds to an allyl anion with one C_1—C_2 bond twisted by 90°: the single isolated AO on C_3 then carries a lone pair and is analogous to the sp^2 (n) orbital of H_2Si=NH; the two AOs on C_1 and C_2 interact to yield the π and π^* orbitals of the C_1=C_2 bond and are analogous to the 3p Si and 2p N AOs of H_2Si=NH that combine to yield its π orbital.

Table II. Electronic Excitation Energies of Silanimines **1–3**

compound	λ_{max}[a] (nm)	f[a,b]	dominant conf.[a,c] (weight, %)	λ_{max}[d] (nm)	f[b,d]	dominant conf.[c,d] (weight, %)
1 calcd[e]	586	0.011	1 → −1 (40)	321	0.0007	2 → −1 (49)
exptl	557					
2 calcd[e]	351	0.014	1 → −1 (40)	318	0.150	2 → −1 (40)
exptl	406					
3 calcd[e]	341	0.069	1 → −1 (36)	297	0.056	2 → −1 (36)
			2 → −1 (16)			1 → −1 (16)
exptl	397					
Me_2Si=NMe calcd	259	0	1 → −1 (49)	195	0.221	2 → −1 (40)

[a] Lowest energy singlet–singlet transition. [b] Oscillator strength. [c] The dominant singly excited configuration and its weight in parentheses. The highest occupied MO is labeled 1, the next lower one 2. The lowest unoccupied MO is labeled −1. [d] The next higher energy singlet–singlet transition. [e] The vertical excitation energy computed at the CIS/DZ+d level at a RHF/6-31G* geometry.

The twisting of the Si=N bond causes all three AOs to interact. It corresponds to a simultaneous gradual untwisting of the C_1—C_2 and twisting of the C_2—C_3 bond of the allyl. When an orthogonally twisted Si=N bond is reached, its 3p Si and sp^2 N orbitals interact, while the 2p N AO is isolated and carries a lone pair. This corresponds to a full planarization of the C_1—C_2 and an orthogonal twist of the C_2—C_3 bond of the allyl anion. Although the n, π, and π^* notation is appropriate only for the planar H_2Si=NH molecule, it is convenient to keep these labels even at the twisted geometries.

At the planar equilibrium geometry, the lowest excited singlet state of H_2Si=NH is calculated[26] to be of $n\pi^*$ nature (λ_{max} = 318 nm). The next one is calculated to be of $\pi\pi^*$ nature (λ_{max} = 238 nm). No calculations of comparable quality are available for Me_2Si=NMe, in which the n $\rightarrow \pi^*$ transition could be expected to be blue-shifted and the $\pi \rightarrow \pi^*$ transition red-shifted. At a much poorer level of calculation, CIS/DZ+d, its vertical n $\rightarrow \pi^*$ transition is calculated at 259 nm and the vertical $\pi \rightarrow \pi^*$ transition at 195 nm (Table II).

Upon twisting, one expects the n $\rightarrow \pi^*$ transition to drop in energy as the highest occupied MO gradually turns into a 2p N lone pair, much higher in energy than the sp^2 N lone pair of the planar structure. This qualitative expectation is reproduced by our rather approximate CIS/DZ+d calculation (Figure 3, Table II). The nature of the excited state wave functions for the lowest two excited singlets is as expected from the simple evaluation of the response to twisting. The computations match the observed trend in the excitation energies of the silanimines amazingly well. In particular, the small difference between **2** and **3**, which differed significantly in their Si=N stretching frequencies, is well reproduced, as is the huge jump upon going to **1**. Once again, these trends are the same as in the carbon analogues, where the observed n $\rightarrow \pi^*$ transition energies are 403, 283, and 287 nm for the analogues of **1**, **2**, and **3**, respectively.[23]

Conclusions. The generation and trapping of the bridgehead silanimines **1–3** have cleared up a puzzle[8] concerning the mechanism of Curtius-type rearrangements of silyl azides. The IR and UV–vis spectra of the matrix-isolated species represent the first direct observations of molecules with twisted Si=N bonds. Both types of spectral results are qualitatively similar to those

(26) Bruna, P. J.; Krumbach, V.; Peyerimhoff, S. D. *Can. J. Chem.* **1985**, *63*, 1594.

observed earlier for carbon analogues with twisted C=N bonds and have been accounted for by *ab initio* calculations to a very satisfactory degree. Although the trends leave no doubt about the importance of π bonding in the electronic structure of the Si=N double bond, they are not easily predictable from the combined effects of double-bond twisting and pyramidalization derived from the calculated structures.

Experimental Section and Calculations

Matrix Isolation. Low-temperature samples were prepared on CsI windows mounted on the cold tip of an APD Cryogenics helium refrigerator. Azides were distilled at −25 °C from a side finger in a stream of Ar and condensed on the cold target kept at 27 K. The matrix ratio was approximately 1:700. Infrared absorption spectra were obtained at 0.5-cm^{-1} resolution on a Nicolet 60-SXR FTIR spectrometer. UV–visible absorption spectra were measured at 0.5-nm resolution on a Varian Cary 5 spectrophotometer. In selective photochemical transformations, we used excimer lasers (Lambda Physik) and an Ar ion/ring-dye laser (Coherent). In the chemical trapping experiments, trimethoxymethylsilane was sprayed on the surface of the matrix after all the desired photochemical transformations and spectroscopic measurements were completed. The matrix was then warmed to room temperature rapidly by filling the cryostat vacuum shroud with argon. The residue left on the window was analyzed immediately. Attempts to mix the trapping agent with argon prior to irradiation were abandoned after it was determined that its absorption bands tend to obscure spectroscopic observations on the substrates.

Synthesis. Boiling points are uncorrected. Melting points were determined on a Boetius PHMK05 apparatus with a microscope attachment (4 °C/min). NMR spectra were run on a Nicolet NT-360 in $CDCl_3$ solvent unless specified otherwise. Mass spectra were taken on a GCMS HP 5995. High resolution and chemical ionization mass spectra were measured on a VG ZAB-2E spectrometer. Elemental analysis was performed by Atlantic Microlabs, Norcross, GA. Preparative GC separations were done on a 5-ft SE-30 (20% on Chromosorb) column.

Tetrahydropyran-4-carboxylic Acid[11] (11). Sodium metal (102 g, 4.44 mol) was dissolved in dry ethanol (1600 mL), diethyl malonate (345 g, 2.15 mol) was added in one portion, and after 10 min, 2-chloroethyl ether (305 g, 2.13 mol) was added over 15 min. The reaction mixture was stirred, refluxed for 10 h, and cooled, and the reaction was quenched with concentrated HCl (20 mL). The inorganic salts were filtered off and washed with ether, and the filtrate was concentrated. The dark residue was vacuum distilled to collect 261 g of the main fraction (bp 80–105 °C (1.0 mmHg); lit.[13] bp 100–105 °C (3.5 mmHg)) containing mostly the diesters and some of the monoester. The distillate was added to a solution of KOH (175 g) in ethanol (1700 mL), and the mixture was stirred and refluxed for 4 h. The resulting hygroscopic dipotassium salt was filtered off, washed with ethanol and diethyl ether, and dried. The potassium salt was dissolved in water (200 mL), and the solution was acidified by slow addition of concentrated HCl (250 mL). The mixture was evaporated to dryness, the solid was washed with acetone (3 × 200mL), the solution was evaporated, and the resulting diacid was carefully pyrolyzed at 190 °C. The crude monoacid (125 g) was short-path distilled (bp 115 °C (0.8 mmHg); lit.[14] bp 144–146 °C (11 mmHg)) to give 115 g (41% overall yield) of white crystals: mp 86–88 °C (lit.[11] mp 89 °C); ^{1}H NMR δ 1.72–1.90 (m, 4H), 2.51–2.60 (m, 1H), 3.34 (dt, J_1 = 11.2 Hz, J_2 = 2.7 Hz, 2H), 3.97 (tm, J = 11.6 Hz, 2H); ^{13}C NMR δ 28.28, 39.70, 66.86, 180.00; EIMS, *m/z* 130 (4, M), 86 (88), 73 (33), 58 (28), 55 (100), 45 (58).

4-(Bromomethyl)tetrahydropyran[15] (12) via Tetrahydropyran-4-methanol 4-Toluenesulfonate. The acid **11** (100 g, 0.77 mol) was slowly added to a stirred suspension of anhydrous potassium carbonate (130 g, 0.80 mol) in acetone (400 mol), followed by dimethyl sulfate (100 g, 0.79 mol). The mixture was stirred and heated for 3 h. The inorganic salts were filtered off and washed with acetone, and the filtrate was dried ($MgSO_4$) and concentrated to give 114.5 g (100% yield) of a yellowish oily ester. The crude ester was dissolved in dry diethyl ether (300 mL) and added dropwise to a stirred suspension of $LiAlH_4$ (18.0 g, 0.47 mol) in diethyl ether (700 mL). The mixture was stirred and refluxed for an additional 3 h, and the reaction was quenched by careful addition of ether saturated with water (410 mL), followed by water (20 mL), 15% NaOH (20 mL), and water (65 mL). The precipitated inorganic salts were filtered off on Celite and washed with a mixture of methanol and ether, and the filtrate was concentrated. The crude product was dissolved in methylene chloride, dried (Na_2SO_4), and evaporated again. The resulting oily alcohol[15] (85 g) was dissolved in dry pyridine (500 mL) and cooled down in an ice bath, and *p*-toluenesulfonyl chloride (200 g, 1.05 mol) was slowly added over a period of 30 min. The mixture was stirred at 0–5 °C for 2 h, then 1 h at room temperature, and poured into a mixture of concentrated HCl (400 mL) and ice (500 g). The precipitated white solid was filtered off and dried to give 190 g of the crude tosylate. An analytical sample of tosylate was obtained by recrystallization from acetone–water: mp 85 °C; ^{1}H NMR δ 1.24 and 1.30 (AB, dd, J_1 = 12.0 Hz, J_2 = 4.4 Hz, 2H), 1.61 (br s, 2H), 1.86–2.01 (m, 1H), 2.45 (s, 3H), 3.34 (td, J_1 = 11.8 Hz, J_2 = 1.8 Hz, 2H), 3.85 (d, J = 6.6 Hz, 2H), 3.94 (dd, J_1 = 11.5 Hz, J_2 = 4.3 Hz, 2H), 7.35 (d, J = 8.2 Hz, 2H), 7.78 (d, J = 8.2 Hz, 2H); ^{13}C NMR δ 21.61 (q), 28.90 (t), 34.64 (d), 67.01 (t), 74.10 (t), 127.68 (d), 129.68 (d), 132.74 (s), 144.63 (s); IR 3029, 2940, 2850, 1598, 1360, 1189, 1176, 1096, 989, 945 cm^{-1}; EIMS, *m/z* 270 (0.3, M), 155 (6), 91 (31), 70 (100), 55 (41). Anal. Calcd for $C_{13}H_{18}O_4S$: C, 57.75; H, 6.71; S, 11.86. Found: C, 57.87; H, 6.71; S, 11.96.

A mixture of the crude tosylate (190 g), potassium bromide (500 g), water (500 mL), and benzyltriethylammonium chloride (3.0 g) was vigorously stirred and refluxed for 5 h. When the starting material was no longer detectable by GC, water was added (500 mL), the organic phase was separated, and the aqueous layer was washed with hexanes. The organic extracts were dried (Na_2SO_4) and evaporated, and the residue (96 g) was distilled (bp 88–90 °C (22 mmHg); lit.[15] bp 84–86 °C (20 mmHg)) to give 78 g (57% overall yield based on acid **11**) of a colorless liquid: ^{1}H NMR δ 1.31 and 1.37 (AB, dd, J_1 = 12.0 Hz, J_2 = 4.5 Hz, 2H), 1.74–1.78 (m, 2H), 1.81–1.98 (m, 1H), 3.28 (d, J = 6.7 Hz, 2H), 3.37 (td, J_1 = 11.9 Hz, J_2 = 1.9 Hz, 2H), 3.98 (dd, J_1 = 11.5 Hz, J_2 = 4.6 Hz, 2H); ^{13}C NMR δ 31.70, 37.55, 38.98, 67.44; IR (neat) 2930, 2845, 1247, 1132, 1096, 1013, 982, 842 cm^{-1}; EIMS, *m/z* 180 (24, M), 178 (26, M), 99 (49), 69 (100), 67 (44), 55 (78), 53 (46).

4-(2-Bromoethyl)tetrahydropyran[17] (13). The bromide was prepared from 4-(bromomethyl)tetrahydropyran (**12**) via 2-(4-tetrahydropyranyl)ethanol[17] which was subsequently converted to the bromide **13**: bp 103–105 °C (22 mmHg) (lit.[16] bp 102 °C (13 mmHg)); ^{1}H NMR δ 1.26 and 1.31 (AB, dd, J_1 = 12.1 Hz, J_2 = 4.4 Hz, 2H), 1.57–1.64 (m, 2H), 1.70–1.87 (m, 3H), 3.38 (td, J_1 = 11.9 Hz, J_2 = 1.8 Hz, 2H), 3.44 (t, J = 6.8 Hz, 2H), 3.95 (dm, J = 11.4 Hz, 2H); ^{13}C NMR δ 30.64, 32.13, 33.16, 39.32, 67.57; IR (neat) 2928, 2841, 1106, 1095 cm^{-1}; EIMS, *m/z* 194 (0.7, M), 193 (0.6, M − 1), 192 (0.8, M), 191 (0.4, M − 1), 113 (37), 95 (20), 55 (100).

1-Chloro-1-silabicyclo[2.2.1]heptane[9] (9). The chloride was obtained in 5.4% overall yield from bromide **12** according to the procedure[18] used for the preparation of 1-chloro-1-silabicyclo[2.2.2]octane. The trichloro compound **14** was obtained in 52% yield (bp 60 °C (1 mmHg); lit.[9] bp 63.5 °C (2 mmHg)). The pentachloro compound **16** was prepared in 26% yield (bp 95 °C (1 mmHg); lit.[9] bp 131 °C (2 mmHg), 50% yield). The cyclization of **16** to the bridgehead chloride **9** was achieved in 40% yield (bp 56 °C (6 mmHg); lit.[9] bp 54 °C (5 mmHg), 45% yield): ^{1}H NMR δ 0.66–0.78 (m, 6H), 1.70–1.87 (m, 4H), 2.26 (br s, 1H); ^{13}C NMR δ 6.29 (t), 17.36 (t), 29.30 (d), 29.78 (t); IR (neat) 2930, 1150, 1052, 830, 820, 786, 707; EIMS, *m/z* 148 (M, 10), 146 (M, 31), 120 (26), 119 (40), 118 (73), 117 (87), 90 (34), 82 (32), 65 (42), 63 (100).

1-Chloro-1-silabicyclo[2.2.2]octane[10] (10). The chloride was prepared from the bromide **13** in 5% overall yield according to the literature procedure.[18] The initial trichloro compound **15** was obtained via the organomagnesium reagent prepared from the bromide **13** (56.0 g, 0.29 mol) and magnesium metal (20.0 g, 0.82 mol) in dry THF (400 mL and 150 mL). No external heat was applied. The Grignard reagent was slowly added (1.5 h) to silicon tetrachloride (300 mL, 438 g, 2.36 mol) in dry THF (200 mL). The resulting salts were filtered off and the residue was distilled (bp 70–75 °C (0.6 mmHg); lit.[18] bp 80–85 °C (0.65 mm Hg)) to give 32.0 g (45% yield) of **15**. The trichloro compound **15** was converted into the pentachloro derivative **17** (bp 100–110 °C (1 mmHg), 53% yield; lit.[10] bp 137.5–138 °C (3.5 mmHg), 80% yield) using boron trichloride solution in hexanes instead of the gaseous reagent. The pentachloro compound **17** was converted into the bridgehead chloride isolated in 22% yield and 85% pure (by GC): bp 65–66 °C (6 mmHg) (lit.[18] bp 62–68 °C (6 mmHg), 27% yield); ^{1}H NMR δ (major peaks) 1.01–1.11 (m, 6H), 1.52 (sep, J = 3.5 Hz, 1H), 1.98–2.06 (m, 6H); ^{13}C NMR δ (major peaks) 9.16 (t, 3C), 27.13 (d), 28.47 (t, 3C); GC–MS, *m/z* 162 (12, M), 160 (31, M), 132 (63), 117 (35), 104 (47), 66 (46), 65 (100).

1-Azido-1-silabicyclo[2.2.1]heptane[8] (4). The chlorosilane **9** (200 mg) was added under an argon atmosphere to a well-stirred suspension of sodium azide (150 mg) in dry acetonitrile (0.5 mL) containing a catalytic

amount of 18-crown-6 ether. The reaction mixture was stirred for 1 h at room temperature. The azide was isolated by preparative GC in 50–70% yield as a colorless oil: ^{1}H NMR δ 0.57–0.67 (m, 6H); 1.67–1.83 (m, 4H), 2.25 (br s, 1H) [lit.[8] ^{1}H NMR (benzene-d_6) δ 0.3 (m, 6H), 1.35 (m, 4H), 1.85 (m, 1H)]; ^{13}C NMR δ 2.26 (t), 15.32 (t), 29.25 (t), 29.36 (d); EIMS, *m/z* 154 (M + 1, 4), 153 (M, 38), 125 (93), 124 (100), 97 (55), 96 (50), 83 (35), 70 (76), 56 (54), 55 (42), 43 (50) [lit.[8] EIMS, *m/z* 153 (M, 72), 125 (100)].

1-[^{15}N]Azido-1-silabicyclo[2.2.1]heptane (4-^{15}N). The azide was prepared as described above, using singly labeled sodium azide ($Na^{14}N^{14}N^{15}N$): EIMS, *m/z* (relative intensity) 155 (M + 1, 4), 154 (M, 34), 126 (93), 125 (100), 98 (44), 97 (33), 83 (37), 71 (80), 57 (31), 56 (33), 55 (42), 43 (50).

Bis(silabicyclo[2.2.1]hept-1-yl) ether. The ether was isolated as a side product in the preparation of the azide **4**: ^{1}H NMR δ 0.39–0.48 (m, 6H), 1.53–1.76 (m, 4H), 2.05 (br, s, 1H); ^{13}C NMR δ 4.23, 14.92, 28.52, 29.63; EIMS, *m/z* 238 (M, 31), 210 (59), 182 (100), 154 (48), 127 (28).

1-Azido-1-silabicyclo[2.2.2]octane[8] (5). The chlorosilane **10** (200 mg) was added under an argon atmosphere to a well-stirred suspension of sodium azide (150 mg) in dry acetonitrile (0.5 mL) containing a catalytic amount of 18-crown-6 ether. The reaction mixture was stirred for 1 h at room temperature. The azide was isolated by preparative GC in 50–70% yield as a colorless oil: ^{1}H NMR δ 0.89–0.94 (m, 6H), 1.51 (sep, J = 3.5 Hz, 1H), 1.95–2.00 (m, 6H) [lit.[8] ^{1}H NMR (CCl_4) δ 0.8 (m, 6H), 1.5 (m, 1H), 1.9 (m, 6H)]; ^{13}C NMR δ 5.79 (t, 3C), 27.31 (d), 27.83 (t, 3C); EIMS, *m/z* 168 (M + 1, 12), 167 (M, 91), 139 (M – N_2, 66), 111 (71), 110 (77), 96 (68), 83 (72), 82 (66), 70 (100), 56 (65), 55 (60), 43 (66) [lit.[8] EIMS, *m/z* 167 (M, 85), 139 (100)].

1-[^{15}N]Azido-1-silabicyclo[2.2.2]octane (5-^{15}N). The azide was prepared from the corresponding silyl chloride **10** and singly labeled sodium azide ($Na^{14}N^{14}N^{15}N$) as described above: EIMS, *m/z* 169 (M + 1, 12), 167 (M, 93), 140 (M – N_2, 60), 112 (61), 111 (48), 110 (48), 97 (49), 96 (42), 84 (36), 83 (62), 82 (66), 71 (100), 57 (43), 56 (55), 55 (62), 53 (31), 43 (66).

Irradiation of Azide 4 in the Presence of Trimethoxymethylsilane.[8] Silyl azide **4** (80 mg) was dissolved in dry cyclohexane (1.0 mL) containing trimethoxymethylsilane[27] (0.20 mL). The mixture was placed in a quartz vessel and irradiated with a XeCl excimer laser (308 nm) for several hours until no starting material was detected by GC. The trapping product was isolated from the reaction mixture by preparative GC (injector and detector, 200 °C; column, 150 °C). The photolysis produced a mixture of two products in a GC-peak intensity ratio of about 3:1, with retention times 38.75 min and 38.86 min (25-ft capillary SE-30 column). On the basis of the relative intensity of distinct multiplets due to $-CH_2N-$ hydrogens and 2D ^{1}H–^{1}H and 2D ^{13}C–^{1}H spectra, the GC signal at 38.75 min was attributed to **8** and the signal at 38.86 min to **6**. The chemical shifts and mass spectra were assigned accordingly, except for the methyl and methoxy groups region: ^{1}H NMR δ 0.10 (s), four major singlets (MeO) with approximately equal area at: 3.45, 3.46, 3.49, 3.55; ^{13}C NMR δ 49.90, 49.97, 51.83, 51.93.

2-Aza-2-(dimethoxymethylsilyl)-1-methoxy-1-silabicyclo[3.2.1]octane (8). 8: ^{1}H NMR δ 0.45–0.60 (m, 4H), 1.37 (m, 1H), 1.50 (m, 1H), 1.65–1.73 (m, 2H), 2.55 (br s, 1H), 2.95 (ddd, J_1 = 13.3 Hz, J_2 = 11.4 Hz, J_3 = 3.8 Hz, 1H), 3.20 (dddd, J_1 = 13.3 Hz, J_2 = 5.6 Hz, J_3 = 3.2 Hz, J_4 = 0.6 Hz, 1H) [lit.[8] ^{1}H NMR δ 0.08 (s, 3H), 0.55 (m, 4H), 1.62 (m, 5H), 3.2 (t, J = 9 Hz, 2H), 3.4 (s, 3H), 3.5 (s, 3H), 3.62 (s, 3H)]; ^{13}C NMR δ –5.97 (q), 4.31 (t), 17.29 (t), 26.05 (t), 33.35 (d), 36.62 (t), 40.82 (t); GC–MSEI (at 38.75 min), *m/z* 262 (M + 1, 5), 261 (M, 21), 246 (M – Me, 62), 232 (40), 218 (46), 192 (32), 191 (31), 105 (33), 75 (53), 59 (100) [lit.[8] EIMS, *m/z* 261 (M, 58), 246 (100)].

2-Aza-2-(dimethoxymethylsilyl)-1-methoxy-1-silabicyclo[2.2.2]octane (6). 6: ^{1}H NMR δ 0.75–0.83 (m, 4H), 1.57 (sep, J = 3.3 Hz, 1H), 1.90 (m, 2H), 2.05 (m, 2H), 3.35 (m, 2H) [lit.[8] ^{1}H NMR δ 0.08 (s, 3H), 0.55 (m, 4H), 1.62 (m, 5H), 3.2 (t, J = 9 Hz, 2H), 3.4 (s, 3H), 3.5 (s, 3H), 3.62 (s, 3H)]; ^{13}C NMR δ –6.41 (q), 8.48 (t, 2C), 27.65 (t, 2C), 30.25 (d); GC–MSEI (at 38.86 min), *m/z* 262 (M + 1, 14), 261 (M, 50), 246 (M – Me, 89), 232 (55), 218 (56), 165 (39), 105 (49), 75 (54), 59 (100) [lit.[8] EIMS, *m/z* 261 (M, 58), 246 (100)].

2-Aza-2-(dimethoxymethylsilyl)-1-methoxy-1-silabicyclo[3.2.2]nonane[8] (7). Irradiation of azide **5** was done as described for azide **4**: ^{1}H NMR δ 0.15 (s, 3H), 0.69–0.77 (m, 2H), 0.81–0.85 (m, 2H), 1.66–1.80 (m, 4H), 1.88–1.95 (m, 2H), 1.99–2.04 (m, 1H), 3.05 (t, J = 5.9 Hz, 2H), 3.44 (s, 3H), 3.50 (s, 6H) [lit.[8] ^{1}H NMR δ 0.1 (s, 3H), 0.75 (m, 4H), 1.76 (m, 7H), 3.0 (m, 2H), 3.35 (s, 3H), 3.47 (s, 6H)]; ^{13}C NMR δ –6.10 (q), 7.66 (t, 2C), 25.80 (t, 2C), 33.18 (d), 39.01 (t), 40.03 (t), 50.10 (q, 2C), 50.43 (q); EIMS, *m/z* 276 (M + 1, 5), 275 (M, 24), 260 (M – Me, 31), 247 (30), 246 (49), 178 (42), 105 (38), 75 (72), 59 (100), 45 (31) [lit.[8] EIMS, *m/z* 275 (M, 64), 260 (100)].

Calculations. IR Spectra. These computations were performed at Nashville using Gaussian 90 and CADPAC programs. Geometries were first optimized with the 3-21G basis set and subsequently with the 6-31G* basis set using the second derivative from the 3-21G calculation. In this way, only five or six optimization cycles were required with the 6-31G* basis set. The second derivatives were obtained analytically. The structure of **1** was first optimized with a C_s symmetry constraint. The optimized structure had one imaginary frequency (54*i* cm^{-1}) and corresponds to a transition state for syn–anti isomerization. Removal of the symmetry constraint permitted us to locate the C_1 minimum.

UV–Vis Spectra. These computations were performed at Boulder using the Gamess program. In order to keep them within manageable limits, they were performed only for the chromophores of **1**, **2**, and **3**, and their irrelevant saturated parts were ignored. This was done by using $Me_2Si{=}NMe$ as a model compound and distorting it so that the C, Si, and N atoms were at positions previously optimized for the ground states of **1**, **2**, or **3**, as described above, and optimizing the positions of the hydrogen atoms. A planar $Me_2Si{=}NMe$ structure, optimized at the RHF/6-31G* level, was also considered for comparison.

CAS–SCF and CI (singles) calculations were performed with Dunning–Hay's double zeta basis set obtained from contracting 9s5p primitive functions, augmented by a single set of polarization functions on the heavy atoms. The active space in the CAS–SCF calculations included four electrons and the HOMO-1, HOMO, LUMO, LUMO+1, and LUMO+2 RHF orbitals. The final CAS–SCF wave functions for all the compounds indicated that the RHF wave function contributes nearly 98% to the ground state. The excited state calculations were therefore performed using the RHF approximation to the ground state of these molecules. The active space for the CI calculations included all the valence occupied, valence virtual, and Rydberg orbitals (excess orbitals from the extended basis set), and the configuration space included all single excitations within the active space. Transition densities were obtained from the converged CI (singles) calculations.

Acknowledgment. We are grateful to the National Science Foundation for research support (CHE 9020896) and an equipment grant (CHE 9022151).

(27) Trimethoxymethylsilane was purchased from Aldrich Chemical Co. and used without further purification: ^{13}C NMR δ –8.78, 50.24.